Device model for the operation of polymer/fullerene bulk heterojunction solar cells

L. J. A. Koster, E. C. P. Smits, V. D. Mihailetchi, and P. W. M. Blom
Materials Science Centre^{Plus}*, University of Groningen, Nijenborgh 4, 9747 AG Groningen, The Netherlands*
(Received 30 June 2004; revised manuscript received 16 March 2005; published 2 August 2005)

We have developed a numerical device model that consistently describes the current-voltage characteristics of polymer:fullerene bulk heterojunction solar cells. Bimolecular recombination and a temperature- and field-dependent generation mechanism of free charges are incorporated. It is demonstrated that in poly[2-methoxy-5-(3′,7′-dimethyloctyloxy)-*p*-phenylene vinylene]- (OC_1C_{10}-PPV-) and [6,6]-phenyl C_{61}-butyric acid methyl ester- (PCBM-) (1:4 wt. %) based solar cells space-charge effects only play a minor role, leading to a relatively constant electric field in the device. Furthermore, at short-circuit conditions only 7% of all free carriers are lost due to bimolecular recombination. The model predicts that an increased hole mobility together with a reduction of the acceptor strength of 0.5 eV will lead to a maximum attainable efficiency of 5.5% in the PPV/PCBM-based solar cells.

DOI: 10.1103/PhysRevB.72.085205 PACS number(s): 72.80.Le, 72.40.+w, 72.20.Jv

I. INTRODUCTION

Organic solar cells based on the bulk heterojunction (BHJ) concept are an auspicious alternative for traditonal silicon-based solar cells, mainly due to their potential for low cost, ease of fabrication, and mechanical flexibility.[1] To make a BHJ, an electron accepting material and an electron donating material are mixed in solution, and subsequently spin cast onto a substrate, thus forming two interpenetrating networks. Light is absorbed in one of the materials (in this study a polymer) and an exciton is created. This exciton dissociates at a donor/acceptor interface, spatially separating the electron and hole which are in two different media now. Next, the charges are transported through the respective percolating networks to the electrodes. In contrast to a BHJ device, a bilayer device has a layered structure, i.e., an electron donating material is deposited on top of an electron accepting material. Since the exciton diffusion length is quite small (typically <10 nm), only light that is absorbed near the junction contributes to the photocurrent. In a BHJ device this problem has been overcome by ensuring that the length scales of both phases are in the order of the exciton diffusion length,[2,3] as evidenced by the strong photoluminescence quenching, which makes the BHJ a more promising concept than the bilayer device layout. However, there are still many questions regarding their operation and processes limiting their performance, which is crucial for optimalization.

In a recent article, Mihailetchi *et al.*[4] have demonstrated that the separation of bound electron-hole pairs into free charges is an important process in solar cells based on poly[2-methoxy-5-(3′,7′-dimethyloctyloxy)-*p*-phenylene vinylene] (OC_1C_{10}-PPV) and [6,6]-phenyl C_{61}-butyric acid methyl ester (PCBM) as donor and acceptor, respectively. At high reverse bias saturation of the photocurrent is observed, indicating that all electron-hole pairs are separated. From this observation it follows directly that at short-circuit conditions only 61% of the electron-hole pairs are dissociated, which is a major loss mechanism in these devices. The importance of other processes such as bimolecular recombination is not known. It has been suggested[5,6] that bimolecular recombination can be excluded because of the (nearly) linear dependence of the short-circuit current on light intensity. It remains to be seen, however, whether this holds only at short-circuit conditions, or at all biases and especially at maximum power output (typically around 0.6 V applied bias).

Goodman and Rose[7] have presented a model for extraction of uniformly photogenerated charges from a photoconductor with noninjecting contacts. In the case of a large difference in mean-free path for electrons and holes, caused by, for example, a large difference in electron and hole mobility, the electric field in the device adjusts itself in such a way that the transport of the slowest carrier is enhanced. This results in a nonuniform field, since the charges of photogenerated electrons and holes do not cancel. Consequently, the slowest charge carrier will dominate the device because the faster carrier can leave the device much easier. In OC_1C_{10}-PPV/PCBM bulk heterojunctions the electron mobility in the PCBM is 1 order of magnitude higher than the hole mobility in OC_1C_{10}-PPV.[8,9] This raises the question of whether the photocurrent will be dominated by a nonuniform electric field and resulting space charge. So far, no detailed description of bulk heterojunction solar cells clarifying field distribution and carrier densities has been given and interpretation of current-voltage curves is often done by using models developed for inorganic *p-n* junctions.[10–13] Recently, Barker *et al.*[14] have presented a numerical model describing the current-voltage characteristics of bilayer conjugated polymer photovoltaic devices. However, since the electronic structures of bilayers and bulk heterojunctions are distinct, their operational principles are fundamentally different.

In this study a device model is presented that quantitatively addresses the role of contacts, drift, and diffusion of charge carriers, charge carrier generation, and recombination. First a brief description of the model is given, followed by an overview of the relevant equations. Subsequently, the generation mechanism of free charge carriers is described, which completes the description of the model. The second part of this article contains details on the numerical scheme, i.e., on the iteration procedure and discretization of the equations. Finally, the results of the simulations are presented, showing field and carrier-denisty distributions for these type of de-

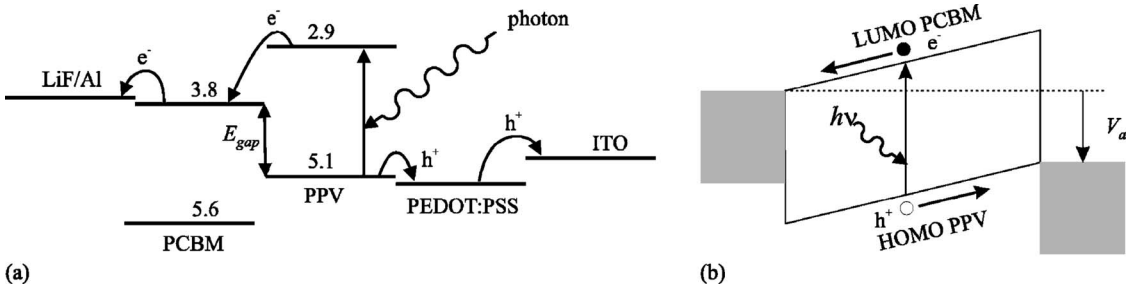

FIG. 1. (a) Schematic of the energy levels (energies given in eV) of the electron donating and electron accepting materials. After charge separation, the electron and hole are transported through the respective materials and collected by the electrodes. As the anode a layer of poly(3,4-ethylenedioxythiophene)/poly(styrenesulfonate) (PEDOT/PSS) deposited on top of indium-tin-oxide (ITO) was used, while on top of the active layer lithium fluoride and aluminum were deposited by thermal evaporation under vacuum. (b) The resulting device model in the metal-insulator-metal representation with positive applied bias V_a, under operating conditions (V_a smaller than open-circuit voltage).

vices. An important loss process in solar cells is the bimolecular recombination of free charge carriers. Our simulations show that the recombination losses in BHJ solar cells strongly depend on the bias conditions; at short circuit only 7% of the free charge carriers is lost due to bimolecular recombination. At the maximum power output, however, the losses increase to 25% due to the decrease of the internal electric field.

II. MODEL

The device is described by using the metal-insulator-metal picture.[15] This means that the device is thought of to be builtup by one semiconductor with the lowest unoccupied molecular orbital (LUMO) of the acceptor and the hightest occupied molecular orbital (HOMO) of the donor as valence and conduction band, respectively, see Fig. 1 for the energy levels of both materials.[11,15] The energy difference between the LUMO of the acceptor and the HOMO of the donor functions as the band gap (E_{gap}) of the semiconductor. Note, that in a disordered system, like an organic solar cell, the band gap will not be a rigorously defined quantity due to the Gaussian density of states of both the acceptor and the donor material.[16]

The model used in this article contains drift and diffusion of charge carriers, and the effect of space charge on the electric field in the device. The resulting basic equations describing transport through semiconductors[17] are solved self-consistently. Recombination is described as a bimolecular process, with the rate given by Langevin.[18] The rate of generation of bound electron-hole pairs is assumed to be homogenous throughout the device. Although this is known not to be strictly correct, the incorporation of an exponential dependence of the generation rate on distance, resulting from absorption of light by the active layer, does not significantly influence our results. As the devices considered in this study are very thin (120 nm), the assumption of uniform generation of electron-hole pairs does not give rise to serious inconsistencies.[19]

The generation of free charge carriers is a two-step process: exciton dissociation across the donor-acceptor interface, which yields a bound electron-hole pair, and subsequent dissociation of this electron-hole pair.[4] The ultrafast (within 100 fs) exciton dissociation, driven by the difference in LUMO levels of OC_1C_{10}-PPV and PCBM, has a quantum efficiency of almost unity[15] and is assumed to be field independent. The resulting electron-hole pair is metastable (up to milliseconds at 80 K) and its dissociation is strongly field and temperature dependent.

In solar cells based on amorphous silicon traps play a dominant role in the description of the solar cell characteristics.[20] In contrast, the current in OC_1C_{10}-PPV based hole-only diodes has been shown to depend quadratic on voltage and exhibit a third power dependence on sample thickness.[21] This behavior is characteristic for a space-charge limited current (SCLC). The occurrence of SCLC enables us to directly determine the hole mobility from the current-voltage characteristics. It should be noted that a material with shallow traps would also exhibit an identical voltage and thickness dependence, and the observed mobility would be an effective mobility in that case, including trapping effects. However, transient measurements demonstrated that the measured mobility does not show any evidence of trapping effects.[22] The same holds true for the electron transport in bulk PCBM.[8] Additionally, the electron and hole mobility in the blend of both materials have been addressed, both showing trap-free SCL current-voltage characteristics.[9,23] Therefore, it can be safely concluded that trapping effects do not play a role in our devices, and hence can be neglected in our model.

A. Basic equations

The basic equations[17] used in this simulation are the Poisson equation

$$\frac{\partial^2}{\partial x^2}\psi(x) = \frac{q}{\varepsilon}[n(x) - p(x)], \tag{1}$$

where q is the elementary charge and ε is the dielectric constant, relating the potential $\psi(x)$ to the electron and hole densities $n(x)$ and $p(x)$, respectively, and the current continuity equations

$$\frac{\partial}{\partial x}J_n(x) = qU(x), \tag{2a}$$

$$\frac{\partial}{\partial x}J_p(x) = -qU(x), \tag{2b}$$

where $J_{n(p)}(x)$ is the electron (hole) current density and $U(x)$ is the net generation rate, i.e., the difference between generation of free carriers and recombination of free carriers. In the remainder of this article, the x dependence of variables is dropped for notational convenience, unless stated otherwise. Only one spatial dimension is considered, since the device has a planar structure with a very small thickness (typically 100 nm) compared to the lateral dimensions (typically several mm).

In order to solve the basic equations, a set of equations is needed relating the current densities to the carrier densities and the potential. Incorporating both drift and diffusion of charge carriers, one has

$$J_n = -qn\mu_n\frac{\partial}{\partial x}\psi + qD_n\frac{\partial}{\partial x}n, \tag{3a}$$

$$J_p = -qp\mu_p\frac{\partial}{\partial x}\psi - qD_p\frac{\partial}{\partial x}p, \tag{3b}$$

where $D_{n,p}$ are the carrier diffusion coefficients, which are assumed to obey the Einstein relation[17]

$$D_{n,p} = \mu_{n,p}V_t, \tag{4}$$

with V_t the thermal voltage, i.e., $V_t = k_BT/q$, where k_B is Boltzmann's constant and T is the absolute temperature. However, we note that at high carrier densities the diffusion coefficient may be increased.[24]

To obtain a unique solution of the system of equations formed by Eqs. (1)–(4) it is necessary to specify the carrier densities and potential at both contacts. The contact at $x=0$, where x denotes the position within the device, will be called the top contact and the contact at $x=L$, where L is the device thickness, the bottom contact. The top contact is assumed to line up with the conduction band of the semiconductor and is therefore Ohmic. Using Boltzmann statistics

$$n(0) = N_c, \tag{5a}$$

$$p(0) = N_c\exp\left(-\frac{E_{\text{gap}}}{V_t}\right), \tag{5b}$$

where N_c is the effective density of states of both the conduction and valence band. This implies that the contacts are in thermodynamic equilibrium, in contrast to the rest of the device. Since the exact values of the effective densities of states of valence and conduction band are not known and are of little importance, one value for both bands is used. Similarly, the bottom contact is assumed to be hole Ohmic, thus

$$n(L) = N_c\exp\left(-\frac{E_{\text{gap}}}{V_t}\right), \tag{6a}$$

$$p(L) = N_c. \tag{6b}$$

The Ohmic nature of both contacts is evidenced by current-voltage measurements on both materials, which clearly show space-charge limited behavior.[8,9] The boundary condition for the potential reads

$$\psi(L) - \psi(0) = E_{\text{gap}} - V_a, \tag{7}$$

where V_a is the applied voltage.

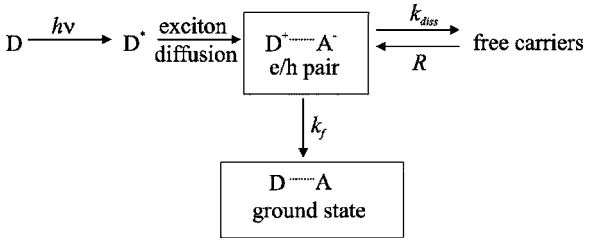

FIG. 2. Schematic of the charge carrier separation at the interface between donor (D) and acceptor (A). Upon excitation of the donor, an exciton is created which diffuses through the donor until it reaches the interface. At the interface, the electron is transfered to the acceptor, thus forming a bound electron-hole pair. This pair can either dissociate into free carriers or decay to the ground state.

B. Generation and recombination

The photogeneration of free charge carriers has been explained by the geminate recombination theory of Onsager.[25] Braun[26] has made an important refinement to this theory by pointing out that the bound electron-hole pair, which acts as a precursor for free charge carriers, has a finite lifetime, see Fig. 2. The bound electron-hole pair may decay to the ground state with a decay rate k_f or dissociate into free carriers. The separation into free carriers is a competition between dissociation (rate constant k_{diss}) and recombination (rate constant R), which revives the charge transfer state.

In Braun's model the probability of electron-hole pair dissociation, for a given electron-hole pair distance x, is given by

$$p(x,T,F) = \frac{k_{\text{diss}}(x,T,F)}{k_{\text{diss}}(x,T,F) + k_f(T)}, \tag{8}$$

depending on both temperature T and field strength F. Based on Onsager's theory for field-dependent dissociation rate constants for weak electrolytes,[27] Braun derives the following expression for k_{diss}:

$$k_{\text{diss}}(x,T,F) = \frac{3R}{4\pi a^3}e^{-E_B/k_BT}J_1(2\sqrt{-2b})/\sqrt{-2b}$$
$$= \frac{3R}{4\pi a^3}e^{-E_B/k_BT}(1 + b + b^2/3 + \cdots), \tag{9}$$

where E_B is the electron-hole pair binding energy $b = q^3F/(8\pi\varepsilon k_B^2T^2)$, F is the field strength, and J_1 is the Bessel function of order 1. For the recombination rate R bimolecular recombination is used,

$$R = \gamma(np - n_{\text{int}}^2), \tag{10}$$

where $n_{\text{int}} = N_c\exp(-E_{\text{gap}}/2V_t)$, is the intrinsic carrier density of electrons and holes. The recombination strength γ is given by the Langevin[18]

$$\gamma = \frac{q}{\langle \varepsilon \rangle} \langle \mu \rangle, \tag{11}$$

where $\langle \mu \rangle$ is the spatially averaged sum of hole and electron mobilities and $\langle \varepsilon \rangle$ is the spatially averaged dielectric constant.[26] The decay rate of the bound electron-hole pair to the ground state, k_f, is used as a fit parameter. As polymer systems are subject to disorder, it is reasonable to assume that the electron-hole pair distance is not constant throughout the system.[28] As a result, Eq. (8) should be integrated over a distribution of separation distances

$$P(a,T,F) = \int_0^\infty p(x,T,F) f(a,x) dx, \tag{12}$$

where $f(a,x)$ is a normalized distribution function given by[4]

$$f(a,x) = \frac{4}{\sqrt{\pi} a^3} x^2 e^{-x^2/a^2}. \tag{13}$$

In the remainder of this article the a,T,F dependencies of P are dropped for notational convenience.

Suppose that G is the generation rate of bound electron-hole pairs. Then the number X of bound electron-hole pairs per unit volume is changed in time by

$$\frac{dX}{dt} = G - k_f X - k_{\text{diss}} X + R. \tag{14}$$

The same equation was used by Barker *et al.*,[14] when they considered dissociation of bound charge carrier pairs in a bilayer photovoltaic device. In steady-state this works out to be

$$G - k_f X = k_{\text{diss}} X - R, \tag{15}$$

which is the net number density of generated free carriers. Therefore, the continuity equation for electrons will read

$$\frac{dn}{dt} = \frac{1}{q} \frac{\partial}{\partial x} J_n + k_{\text{diss}} X - R. \tag{16}$$

Using Eq. (8), $k_{\text{diss}} = [P/(1-P)] k_f$, therefore, Eq. (15) becomes

$$k_{\text{diss}} X = PG + PR \tag{17}$$

and finally the continuity equation becomes

$$\frac{1}{q} \frac{\partial}{\partial x} J_n = PG - (1-P) R. \tag{18}$$

This implies that after bimolecular recombination the carriers are not neccesarily lost, but first form a bound electron-hole pair, which can either again dissociate into free carriers or decay to the ground state, in which case the carriers are lost. Finally, the net generation rate becomes

$$U = PG - (1-P) \gamma (np - n_{\text{int}}^2). \tag{19}$$

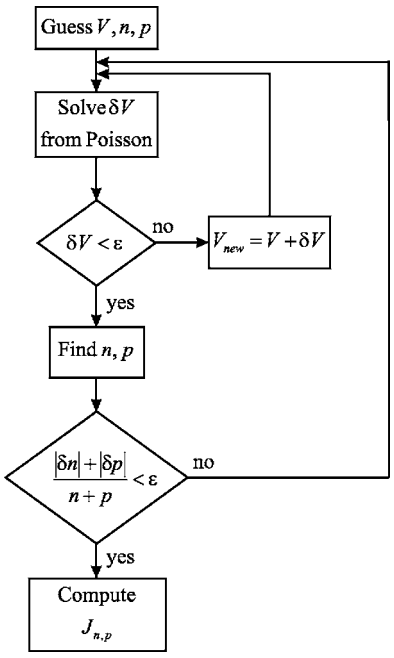

FIG. 3. Flow diagram of the simulation program. To solve the basic equations, Gummel iteration is used. First a guess is made for the potential and carrier densities. Subsequently, a correction $\delta\psi$ to the guess for the potential is calculated from the Poisson equation. This correction is added to the guessed potential and this is repeated until convergence is reached. Next, the carrier densities are calculated from the new potential by solving the continuity equations. This entire procedure is repeated until the change in the carrier densities becomes very small, i.e., until convergence is reached.

III. NUMERICAL METHOD

A. Iteration scheme

The scheme used to solve the Poisson and continuity equations is based on the work of Gummel.[29] In this scheme, first a guess is made for the potential and the carrier densities. With this guess, a correction $\delta\psi$ to the guessed potential is calculated from the Poisson equation. This new potential is then used to update the carrier densities by solving the continuity equations. This process is repeated until convergence is reached. A flow diagram of this method is shown in Fig. 3.

B. Discretization

The basic equations are discretized on a finite number of points, thus giving a finite number of equations. The set of these points forms the grid, which is specified by $h_i = (x_{i+1} - x_i)$, where i is the index of the grid point. To discretize the basic equations, the method of finite differences is used.[17] In this method all derivatives are replaced by differences between grid points, e.g.,

$$\frac{\partial}{\partial x} \psi \Big|_i \approx \frac{\psi_{i+1/2} - \psi_{i-1/2}}{\frac{h_i + h_{i-1}}{2}}. \tag{20}$$

Discretization of the continuity equations requires a little care since it is necessary to approximate the carrier densities

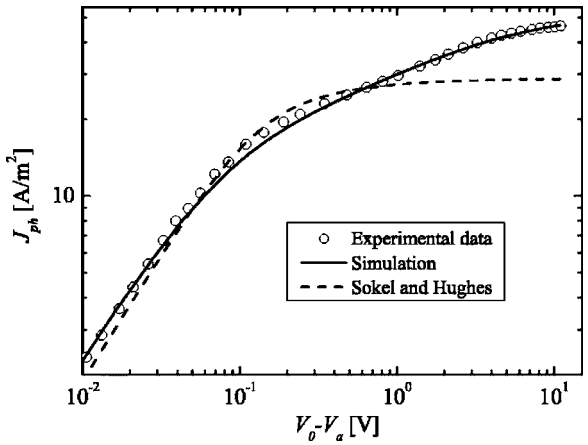

FIG. 4. Photocurrent density J_{ph} as a function of effective applied voltage (V_0-V_a). The symbols represent experimental data of OC_1C_{10}-PPV/PCBM devices at room temperature. The solid line denotes the simulation, while the dashed line represents the result of Sokel and Hughes.

between two grid points in order to get a finite difference equation due to the first order derivative in Eq. (2). Simply approximating the carrier densities by averaging between grid points can lead to serious instabilities since the carrier concentrations can vary very rapidly between grid points. Scharfetter and Gummel[30] have proposed a solution to this problem. In their approach the field is assumed constant between grid points and an exponential variation of the carrier densities results. For example, one has for the electron density

$$n(x \in [x_i, x_{i+1}]) = [1 - g_i(x,\psi)]n_i + g_i(x,\psi)n_{i+1}, \quad (21)$$

where the growth function $g_i(x,\psi)$ is defined as

$$g_i(x,\psi) = \frac{1 - \exp\left(\frac{\psi_{i+1} - \psi_i}{V_t}\frac{x - x_i}{h_i}\right)}{1 - \exp\left(\frac{\psi_{i+1} - \psi_i}{V_t}\right)}. \quad (22)$$

A similar expression holds for the hole density.

IV. SIMULATION RESULTS AND DISCUSSION

A. Comparison with experimental data

In Fig. 4 the experimental data obtained from current-voltage measurements performed on 120-nm-thick OC_1C_{10}-PPV/PCBM (20:80 wt. %) bulk heterojunction solar cells are displayed. In this graph the effective photocurrent density J_{ph}, obtained by subtracting the dark current from the current under illumination, is plotted as a function of effective applied voltage V_0-V_a, where V_0 is the compensation voltage at which $J_{\mathrm{ph}}=0$.[4] In this way, V_0-V_a reflects the internal electric field in the device. It should be noted that $V_a=0.884$ V is very close to the open-circuit voltage (0.848 V). The measurements were performed at room temperature in a nitrogen atmosphere. A white halogen lamp, set to approximately 800 W/m^2, was used to illuminate the devices. For low effective voltages V_0-V_a the photocurrent increases linearly with effective voltage, and subsequently tends to saturate. Mihailetchi *et al.*[4] demonstrated that this low voltage part can be described with an analytical model developed by Sokel and Hughes[31] for zero recombination, as indicated by the dashed line in Fig. 4. The linear behavior at low effective voltage is the result of a direct competition between diffusion and drift currents. At highter effective voltage all free charge carriers are extracted for zero recombination and the photocurrent saturates to qGL. The fact that the experimental photocurrent does not saturate at qGL, but gradually increases for large effective voltages has been attributed to the field dependence of the generation rate G. The two parameters governing the field- and temperature-dependent generation rate, the electron-hole pair distance a and the decay rate k_f, could be estimated by equating the high field photocurrents to qGL.

TABLE I. Overview of the parameters used in the fit to the data shown in Figs. 4 and 5.

Parameter	Symbol	Numerical value
Band gap	E_{gap}	1.34 eV
Electron mobility	μ_n	2.5×10^{-7} m^2/V s
Hole mobility	μ_p	3.0×10^{-8} m^2/V s
Eff. density of states	N_c	2.5×10^{25} m^{-3}
Generation rate	G	2.7×10^{27} m^{-3}
Dielectric constant	$\langle\varepsilon\rangle$	3.0×10^{-11} F/m
e/h Pair distance	a	1.3 nm
Decay rate	k_f	1.5×10^{6} s^{-1}

The device model presented in this paper additionally includes the effects of space-charge and recombination. In Fig. 4 a fit to the experimental data is shown covering a large effective voltage range of $10^{-2}-10$ V. All parameters used in this fit are listed in Table I. The values for the electron- and hole mobilty are obtained experimentally (respectively, 2×10^{-7} m^2/V s and 2×10^{-8} m^2/V s).[8,9] It should be noted that the value of the electron-hole pair separation distance a determines the field at which the dissociation efficiency saturates, and hence a can be determined indepently of k_f. It appears from Fig. 4 that the calculated photocurrent fits the experimental data over the entire voltage range. For comparison, in Fig. 5 the experimental and calculated photocurrent are also shown in a conventional linear plot focusing on the fourth quadrant. The excellent agreement between experimental and calculated data now allows us to further analyze the device behavior in more detail under different bias conditions.

B. The device at short circuit

The calculated potential, current densities, carrier densities, and net generation rate at short circuit (SC) are depicted in Fig. 6. The potential under illumination is virtually equal to the potential in dark (not shown). While Ohmic contacts do not inject charge at this bias, the carrier density at the contacts is very large. The number of photogenerated charges

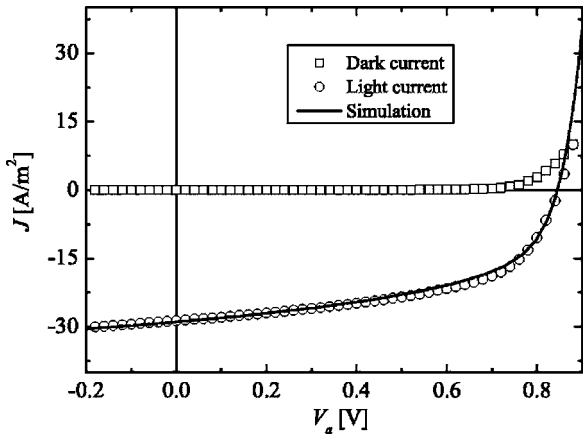

FIG. 5. Experimental dark (squares) and light current (circles) of an OC_1C_{10}-PPV/PCBM device at room temperature. The solid line denotes the simulation.

is not sufficient to change the potential significantly. Apart from band bending near the contacts, a consequence of the large amount of charge, the field is constant throughout the device and concomitantly so is the dissociation rate. As a result, the current densities exhibit a linear dependence on the position in the device. The only exception to this is found near the contacts where both electron and hole densities are high, especially near the top contact ($x=0$), and recombination becomes important.

In the bulk of the device, the hole density is roughly 1 order of magnitude higher than the electron density. This is a result of the difference in mobility between electrons and holes. Since the holes are much slower, they pile up in the device. If the difference in mobility becomes large enough, then the hole density will become so large that the potential under illumination differs from the potential in dark, due to space charge. However, with a mobility difference of only a factor of ten, the overall carrier densities are rather low as compared to other devices like LEDs or FETs. This is because the field in the device is quite large at SC and carriers are readily extracted. For this reason space-charge effects only play a minor role, leading to a nearly constant field in the device.

The average dissociation rate $\langle P\rangle$ of bound electron-hole pairs is equal to 61%.[4] This implies that a significant improvement to the device performance could be made by facilitating this dissociation. The number of charge carriers lost due to recombination can be computed in the following way. The average net generation rate $\langle U\rangle$ can be obtained by integrating Eq. (2a), which yields

$$\langle U\rangle = \frac{1}{L}\int_0^L U(x)dx = \frac{J_n(L) - J_n(0)}{qL}. \tag{23}$$

The total number of generated charges is calculated from the average dissociation rate and whence the recombination rate is known. It turns out that at short-circuit conditions only 7.0% of the free charge carriers are lost due to bimolecular recombination and subsequent decay. These low recombination losses are in agreement with the experimental observation that the short-circuit current exhibits a nearly linear dependence on light intensity.[5,6] The low loss of charge carriers is a consequence of the high field strength, which ensures good charge extraction, resulting in low carrier densities at SC. Since the carrier densities are low, bimolecular recombination is weak and hence the recombination lifetime of the charge carriers is relatively long. On the other hand, due to the high field strength, the time needed for the charge carriers to exit the device is quite small, and therefore only few charge carriers are lost. An overview of dissociation rate and loss of carriers at various applied voltages is given in Table II.

TABLE II. An overview of voltage, current density, average dissociation probability, and relative number of free carriers lost due to recombination at short-circuit (SC), maximum power (MP), and open-circuit (OC) conditions.

	V_a (V)	J (A/m^2)	$\langle P\rangle$ %	rec. loss %
SC	0	29.0	61.0	7.0
MP	0.653	19.5	51.5	24.9
OC	0.846	0	47.4	97.8

C. The device at maximum power output

The maximum power (MP) output is found at $V_a = 0.653$ V for the simulated device. At this bias, the field in

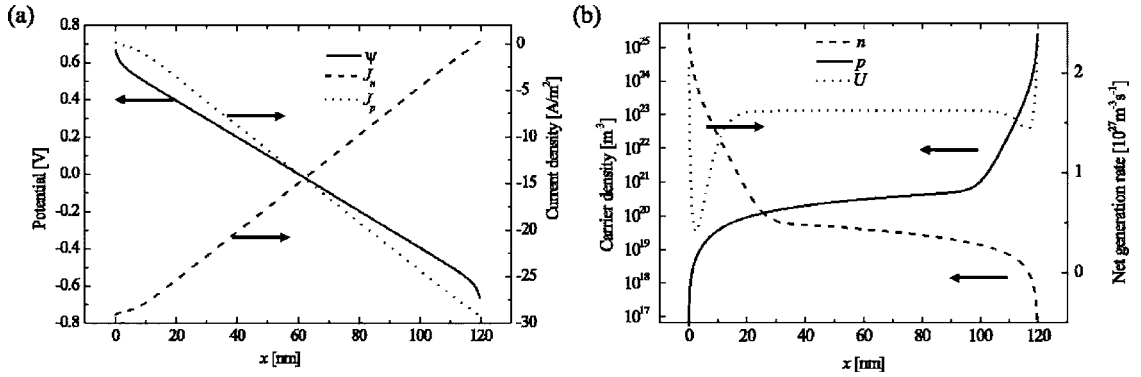

FIG. 6. The device at short circuit, (a) shows the potential and current densities, (b) shows the carrier densities and the net generation rate.

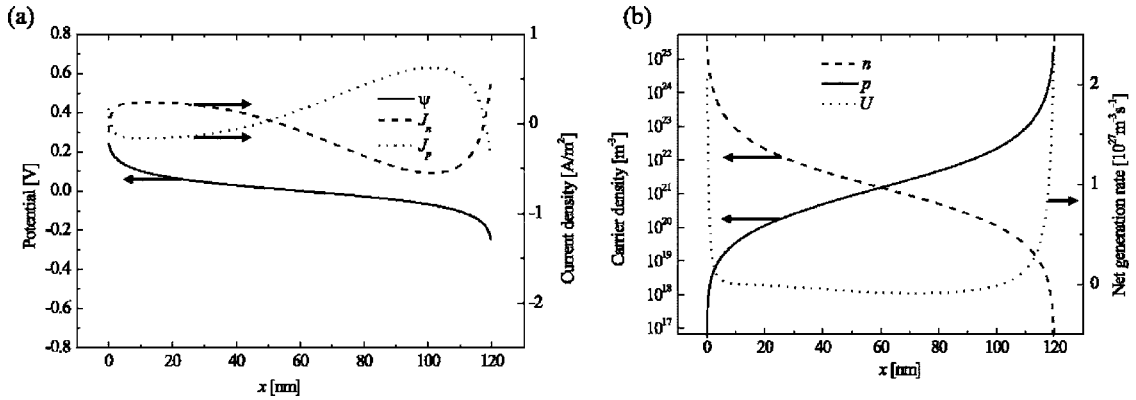

FIG. 7. The device at open circuit, (a) shows the potential and current densities, (b) shows the carrier densities and the net generation rate. Note that the scale on the right-hand side of (a) is enlarged as compared to Fig. 6(a).

the device is smaller than at SC, resulting in a smaller dissociation efficiency being 51.5%, see Table II. Another consequence of the reduction of the field strength is the increase of lost free carriers, as much as 24.9% of all free carriers recombine and subsequently decay. This increase of losses is for the largest part a consequence of a less favorable extraction of charges. First, the time it takes for a charge carrier to exit the device is longer as compared to SC, due to a lower electric field strength in the device. This leads to larger charge carrier densities, thereby increasing the probability of bimolecular recombination of charge carriers. Furthermore, the dissociation probability of a bound electron-hole pair slightly decreases, leading to larger loss of carriers once bimolecular recombination has taken place.

D. The device at open circuit

At open-circuit (OC) conditions, it is evident that the field in the device is smaller than at SC, see Fig. 7. Since there is no net current, there exists a balance between drift and diffusion of charge carriers. Therefore, the field in the device cannot be zero and, consequently, the OC voltage is smaller than the band gap.[32]

The current densities are almost zero throughout the device. The reason for the current densities not being zero everywhere lies in the field dependence of the generation rate. In case of a constant generation rate the current densities would be zero everywhere. From Fig. 7 it can be seen that the densities are almost symmetrical. In fact, if the generation rate would be constant, then from Eq. (3),

$$\frac{1}{V_t}\frac{\partial}{\partial x}\psi = \frac{1}{n}\frac{\partial}{\partial x}n = -\frac{1}{p}\frac{\partial}{\partial x}p. \tag{24}$$

Integration yields

$$\ln\frac{n(x_b)}{n(x_a)} = \ln\frac{p(x_a)}{p(x_b)} \quad \forall\, x_a, x_b \in [0,L] \tag{25}$$

and hence

$$\frac{n(x_b)}{n(x_a)} = \frac{p(x_a)}{p(x_b)}. \tag{26}$$

Using Eqs. (5a) and (6b), we have

$$n(L-x) = p(x), \tag{27}$$

showing that the carrier densities are indeed symmetrical.

Another striking feature of Fig. 7 is the fact that the carrier densities are much higher at OC than at SC. This is because of the much lower field which makes extraction of charge carriers much more difficult. This also results in a much smaller net generation rate, in fact, 97.8% of all free charge carriers are lost due to recombination. Only in the immediate vicinity of the contacts there is a significant net generation of charge carriers. This is not due to an increase in generation due to a higher electric field, but due to the fact that at the contact there is an enormous difference in charge carriers densities and the free carriers have no counter part to recombine with.

E. Comparison with (in)organic low mobility solar cells

Having discussed the device characteristics of polymer/fullerene BHJ cells it is interesting to compare their operating mechanism with other types of solar cells that also employ low mobility semiconductors as amorphous silicon (*a*-Si) based *p-i-n* devices.[33–35] These devices consist of a thin layer of intrinsic material sandwiched between heavily doped *p* and *n* layers, which function as electrodes. First, the photogeneration of charges in these *p-i-n* devices is fundamentally different: light absorption directly creates free charge carriers since geminate recombination of photogenerated charge carriers is of no importance.[36] In a BHJ device an exciton is created upon light aborption, which subsequently dissociates across the donor/acceptor interface, creating a bound electron-hole pair. This bound pair can either dissociate into free charges contributing to the photocurrent

or decay to the ground state, resulting in a strongly field- and temperature-dependent geminate recombination process.[4] This difference is at the heart of our model. Furthermore, bimolecular recombination, and not trapping and subsequent recombination, is the prime loss mechanism of free carriers (i.e., carriers that already escaped the bound electron-hole pair).

The operational principle of dye-sensitized solar cells (DSSCs) has received much attention as well. Such a DSSC consists of a nanoporous titanium dioxide electrode, covered with a monolayer of dye molecules, immersed in a liquid electrolyte containing, e.g., the I^-/I_3^- redox couple.[37] Light is absorbed by the dye layer and consequently, the electrons are transported through the titanium dioxide phase, while the dye molecule is reduced by the I^-/I_3^- redox couple. There has been much debate about whether the driving mechanism of charge transport of these devices is the same as for *p-n* junctions.[38–40] Whereas *p-n* junctions need a built-in field to transport the charges, DSSCs do not seem to need an internal field. Rather, the hole transport through the electrolyte is driven by diffusion, since the electrolyte cannot sustain an electric field. The transport of electrons is less well understood and two models have been proposed:[41] The so-called junction model assumes that electrons are field driven, thereby limiting the open-circuit voltage to the difference in work function of the substate electrode and the solution redox potential. The kinetic model on the other hand, assumes that the electrons are also driven by diffusion, as are the holes, and that the electric field in the titanium dioxide network is zero due to screening by the electrolyte. Therefore, the charge carriers diffuse away from the interface where they were created, and hence an internal electric field is not needed for photovoltaic action. As a result even a device with equal redox potential and substrate electrode workfunction can exhibit a nonzero open-circuit voltage. This has indeed been observed for DSSCs,[41] as well as for bilayer devices consisting of conjugated polymers[42] with top and bottom electrodes with the same work function.

It has been asserted that the same should hold for BHJ devices, but that the electric field must also be taken into account since there is no mobile electrolyte to screen the field.[43,44] As a consequence, the open-circuit should not be limited to the difference in electrode work function. However, by varying the workfunction of the PEDOT:PSS anode, Frohne *et al.* have shown that when the workfunction of the anode coincides with the LUMO of PCBM, thereby yielding a symmetric device, the open-circuit voltage is zero.[45] Furthermore, Mihailetchi *et al.* also demonstrated, by varying the top electrode (cathode), that the open-circuit voltage is determined by the difference in electrode work function.[46] These results are in full agreement with the metal-insulator-metal picture used here. Since we treat the BHJ as one effective semiconductor, there is no interface for the charge carriers to diffuse away from and the transport is modeled as taking place in only one material, thereby resembling the *p-i-n* junction model. The succes of the metal-insulator-metal picture suggests that such diffusion is not important in BHJ solar cells. Not only is this model succesful in describe the effect of various electrodes on the open-circuit voltage,[45,46] it also describes, e.g., its light intensity dependence.[47]

F. Solar cell efficiency

The consistency of the model with the experiments allows us to provide guidelines for the further optimization of the performance of bulk-heterojunction solar cells. Currently, the power conversion efficiency of OC_1C_{10}-PPV/PCBM solar cells (1:4 in weight) is 2.5%.[2] Several factors limit the performance, e.g., poor overlap with the solar spectrum, low hole mobility of OC_1C_{10}-PPV, and the matching of the LUMO levels of OC_1C_{10}-PPV and PCBM. Increasing the OC_1C_{10}-PPV hole mobility to the value of the PCBM electron would increase the efficiency to 3.1%. The origin of this efficiency increase is twofold: First the separation of the boud electron-hole pair becomes more efficient, because it is easier for the hole to escape. Second, at MP the loss of free carriers due to bimolecular recombination is further reduced. A more spectacular increase would result if the LUMO of PCBM was shifted from 3.8 to 3.3 eV, keeping all other parameters the same. The efficiency of polymer/fullerene BJH devices is strongly dependent on the offset between the band-edge positions of the LUMO of the polymer and fullerene. It has been found[48] that a band-edge offset larger than the exciton binding energy of the intrachain singlet excitons (typically 0.4 eV) leads to ionization of the exciton, required for efficient photovoltaic operation. Consequently, the current positioning of the band levels of donor (2.9 eV) and acceptor (3.8 eV) are such that 0.5 eV is lost in the electron-transfer reaction. By more careful positioning, the energy difference between the two LUMOs of 0.9 eV can likely be reduced to 0.4 eV, without a loss in the rate of the forward electron transfer. This critical point has hardly been considered before, yet it allows V_{oc} to be raised from 0.85 to 1.35 V, and an efficiency of 4.5% would be obtained. Combining these two effects would result in an ultimate efficiency of 5.5%.

V. SUMMARY AND CONCLUSIONS

We have developed a numerical model for the current-voltage characteristics of polymer/fullerene bulk heterojunction solar cells. The model includes drift and diffusion of charge carriers, the influence of space charge on the electric field, field- and temperature-dependent generation of free charge carriers, and bimolecular recombination. This model has been used to simulate experimental data of a polymer/fullerene bulk heterojunction photovoltaic device. At SC only 61% of all created bound electron-hole pairs dissociate into free carriers. Once separated though, only 7% of all charge carriers are lost due to bimolecular recombination and subsequent decay. At maximum power output the situation is

different, less electron-hole pairs are separated (52%) and, more importantly, the loss of free carriers is much higher (25%). Therefore, bimolecular recombination, although not important at SC, is a significant loss mechanism in photovoltaic devices. At OC, the charge carrier densities become larger due to the slower extraction of charge carriers. Since the diffusion of charges has to be opposed by drift of charges, the field in the device is nonzero.

ACKNOWLEDGMENTS

The authors thank J. C. Hummelen for supply of the PCBM and fruitful discussions. These investigations were financially supported by the Dutch Ministries of EZ, O&W, and VROM through the EET program (Grant No. EETK97115). The work of L. J. A. Koster forms part of the research program of the Dutch Polymer Institute (Grant No. 323).

[1] Siemens press release, 7 January 2004.
[2] S. E. Shaheen, C. J. Brabec, N. S. Sariciftci, F. Padinger, T. Fromherz, and J. C. Hummelen, Appl. Phys. Lett. **78**, 841 (2001).
[3] J. K. J. van Duren, X. Yang, J. Loos, C. W. T. Bulle-Lieuwma, A. B. Sieval, J. C. Hummelen, and R. A. J. Janssen, Adv. Funct. Mater. **14**, 425 (2004).
[4] V. D. Mihailetchi, L. J. A. Koster, J. C. Hummelen, and P. W. M. Blom, Phys. Rev. Lett. **93**, 216601 (2004).
[5] I. Riedel, J. Parisi, V. Dyakonov, L. Lutsen, D. Vanderzande, and J. C. Hummelen, Adv. Funct. Mater. **14**, 38 (2004).
[6] P. Schilinsky, C. Waldauf, and C. J. Brabec, Appl. Phys. Lett. **81**, 3885 (2002).
[7] A. M. Goodman and A. Rose, J. Appl. Phys. **42**, 2823 (1971).
[8] V. D. Mihailetchi, J. K. J. van Duren, P. W. M. Blom, J. C. Hummelen, R. A. J. Janssen, J. M. Kroon, M. T. Rispens, W. J. H. Verhees, and M. M. Wienk, Adv. Funct. Mater. **13**, 43 (2003).
[9] C. Melzer, E. Koop, V. D. Mihailetchi, and P. W. M. Blom, Adv. Funct. Mater. **14**, 865 (2004).
[10] E. A. Katz, D. Faiman, S. M. Tuladhar, J. M. Kroon, M. M. Wienk, T. Fromherz, F. Padinger, C. J. Brabec, and N. S. Sariciftci, J. Appl. Phys. **90**, 5343 (2001).
[11] V. Dyakonov, Physica E (Amsterdam) **14**, 53 (2002).
[12] C. J. Brabec, S. E. Shaheen, C. Winder, N. S. Sariciftci, and P. Denk, Appl. Phys. Lett. **80**, 1288 (2002).
[13] P. Schilinsky, C. Waldauf, J. Hauch, and C. J. Brabec, J. Appl. Phys. **95**, 2816 (2004).
[14] J. A. Barker, C. M. Ramsdale, and N. C. Greenham, Phys. Rev. B **67**, 075205 (2003).
[15] C. J. Brabec, N. S. Sariciftci, and J. C. Hummelen, Adv. Funct. Mater. **11**, 15 (2001).
[16] H. Bässler, Phys. Status Solidi B **175**, 15 (1993).
[17] S. Selberherr, *Analysis and Simulation of Semiconductor Devices* (Springer-Verlag, Wien, Germany, 1984).
[18] P. Langevin, Ann. Chim. Phys. **28**, 433 (1903).
[19] H. Hoppe, N. Arnold, D. Meissner, and N. S. Sariciftci, Thin Solid Films **451–452**, 589 (2004).
[20] M. A. Green, *Solar Cells Operating Principles, Technology and System Applications* (Prentice Hall, Englewood Cliffs, NJ, 1982).
[21] P. W. M. Blom, M. J. M. de Jong, and J. J. M. Vleggaar, Appl. Phys. Lett. **68**, 3308 (1996).
[22] J. C. Scott, S. Ramos, and G. G. Malliaras, J. Imaging Sci. Technol. **43**, 234 (1999).
[23] V. D. Mihailetchi, L. J. A. Koster, P. W. M. Blom, C. Melzer, B. de Boer, J. K. J. van Duren, and R. A. J. Janssen, Adv. Funct. Mater. **15**, 795 (2005).
[24] Y. Roichmann and N. Tessler, Appl. Phys. Lett. **80**, 1948 (2002).
[25] L. Onsager, Phys. Rev. **54**, 554 (1938).
[26] C. L. Braun, J. Chem. Phys. **80**, 4157 (1984).
[27] L. Onsager, J. Phys. Chem. **2**, 599 (1934).
[28] T. E. Goliber and J. H. Perlstein, J. Chem. Phys. **80**, 4162 (1984).
[29] H. K. Gummel, IEEE Trans. Electron Devices **11**, 455 (1964).
[30] D. L. Scharfetter and H. K. Gummel, IEEE Trans. Electron Devices **16**, 64 (1969).
[31] R. Sokel and R. C. Hughes, J. Appl. Phys. **53**, 7414 (1982).
[32] V. D. Mihailetchi, P. W. M. Blom, J. C. Hummelen, and M. T. Rispens, J. Appl. Phys. **94**, 6849 (2003).
[33] E. A. Schiff, Sol. Energy Mater. Sol. Cells **78**, 567 (2003).
[34] P. Chatterjee, J. Appl. Phys. **76**, 1301 (1994).
[35] F. A. Rubinelli, R. Jiménez, J. K. Rath, and R. E. I. Schropp, J. Appl. Phys. **91**, 2409 (2002).
[36] F. Carasco and W. E. Spear, Philos. Mag. B **47**, 495 (1983).
[37] M. Grätzel, Prog. Photovoltaics **8**, 171 (2000).
[38] K. Schwarzburg and F. Willig, J. Phys. Chem. B **107**, 3552 (2003).
[39] G. Kron, T. Egerter, J. H. Werner, and U. Rau, J. Phys. Chem. B **107**, 3556 (2003).
[40] B. A. Gregg, J. Phys. Chem. B **107**, 13540 (2003);J. Bisquert, *ibid.* **107**, 13541 (2003);J. Augustynski, *ibid.* **107**, 13544 (2003);K. Schwarzburg and F. Willig, *ibid.* **107**, 13546 (2003);U. Rau, G. Kron , and J. H. Werner, *ibid.* **107**, 13547 (2003);
[41] F. Pichot and B. A. Gregg, J. Phys. Chem. B **104**, 6 (2000).
[42] C. M. Ramsdale, J. A. Barker, A. C. Arias, J. D. MacKenzie, R. H. Friend, and N. C. Greenham, J. Appl. Phys. **92**, 4266 (2002).
[43] B. A. Gregg and M. C. Hanna, J. Appl. Phys. **93**, 3605 (2003).
[44] B. A. Gregg, J. Phys. Chem. B **107**, 4688 (2003).
[45] H. Frohne, S. E. Shaheen, C. J. Brabec, D. C. Müller, N. S. Sariciftci, and K. Meerholz, ChemPhysChem **9**, 795 (2002).
[46] V. D. Mihailetchi, P. W. M. Blom, J. C. Hummelen, and M. T. Rispens, J. Appl. Phys. **94**, 6849 (2003).
[47] L. J. A. Koster, V. D. Mihailetchi, R. Ramaker, and P. W. M. Blom, Appl. Phys. Lett. **86**, 123509 (2005).
[48] J. J. M. Halls, J. Cornil, D. A. dos Santos, R. Silbey, D. H. Hwang, A. B. Holmes, J. L. Bredas, and R. H. Friend, Phys. Rev. B **60**, 5721 (1999).